



Published in final edited form as:

Oncogene. 2013 January 24; 32(4): 444–452. doi:10.1038/onc.2012.71.

UVB-induced COX-2 expression requires histone H3 phosphorylation at Ser10 and Ser28

Young-Sam Keum^{1,3}, Hong-Gyum Kim¹, Ann M. Bode¹, Young-Joon Surh², and Zigang Dong^{1,2}

¹The Hormel Institute, University of Minnesota, 801 16th Ave NE, Austin, MN 55912

²WCU Program, Department of Molecular Medicine and Biopharmaceutical Chemistry, Graduate School of Convergence Science and Technology and College of Medicine, Seoul National University, Seoul, South Korea 151-742

³Department of Biochemistry, College of Pharmacy, Dongguk University, 813 Siksa-dong, Goyang, South Korea 410-773

Abstract

Cyclooxygenase-2 (COX-2) is an inducible enzyme that contributes to the generation of chronic inflammation in response to chemical carcinogens and environmental stresses, including ultraviolet B (UVB) irradiation. Although post-translational histone modifications are believed to play an important role in modulating transcriptional regulation of UVB-induced COX-2, the underlying biochemical mechanisms are completely unknown. Here, we show that UVB activates the p38 MAPK/MSK1 kinase cascade to phosphorylate histone H3 at Ser10 and Ser28, contributing to UVB-induced COX-2 expression. UVB has no effect on the global trimethylation level of histone H3 (H3K4me3, H3K9me3, and H3K27me3). We observed that selected mammalian 14-3-3 proteins bind to UVB-induced phosphorylated histone H3 (Ser10 and Ser28). In particular, 14-3-3ε is critical for recruiting MSK1 and Cdk9 to the chromatin and subsequently phosphorylating the C-terminal domain (CTD) of RNA polymerase II in the *cox-2* promoter. We propose that histone H3 phosphorylation at Ser10 and Ser28 serve as critical switches to promote *cox-2* gene expression by facilitating the recruitment of MSK1 and Cdk9 to the *cox-2* promoter, thereby promoting RNA polymerase II phosphorylation.

Keywords

COX-2; UVB; histone H3; phosphorylation; Cdk9; RNA polymerase II

Users may view, print, copy, download and text and data- mine the content in such documents, for the purposes of academic research, subject always to the full Conditions of use: http://www.nature.com/authors/editorial_policies/license.html#terms

Correspondence to Zigang Dong, The Hormel Institute University of Minnesota, 801 16th Ave NE, Austin, MN 55912; zgdong@hi.umn.edu; telephone 507-437-9600; FAX 507-437-9606 .

Conflict of Interest All the authors declare no conflict of interest.

Introduction

Cyclooxygenases (COX) are enzymes that catalyze the rate-limiting conversion of arachidonic acid into bioactive lipids, such as the prostaglandins, prostacyclins and thromboxanes. Two major forms of COX, COX-1 and COX-2, exist and each is encoded by a separate gene. Whereas COX-1 is constitutively expressed and stable in most tissues, COX-2 is barely detectable, but highly inducible in response to mitogens, pro-inflammatory cytokines, growth factors, hormones, tumor promoters and environmental stresses (1). The induction of COX-2 is implicated in many inflammation-associated chronic disorders and serves as a major biochemical mechanism that contributes to UVB-induced skin carcinogenesis (2). The intracellular signaling kinase pathways involving UVB irradiation and the induction of COX-2 protein expression in skin have been fairly well elucidated with a vast amount of *in vivo* and *in vitro* experimental evidence. UVB exposure causes a generation of intracellular reactive oxygen species (ROS) and phosphorylation of epidermal growth factor receptor (EGFR) that, in turn, activates two major intracellular signaling kinase cascades. These cascades include the mitogen-activated protein kinase (MAPK) and phosphatidylinositol 3-kinase (PI3-K) pathways. The stimulation of these pathways results in the activation of COX-2 transcription factors, including nuclear factor kappaB (NF- κ B), activator protein-1 (AP-1), cAMP response element-binding protein (CREB), and activating transcription factor-1 (ATF1) (3). UVB can also induce COX-2 transcriptional activation by enhancing *cox-2* mRNA stability, but the detailed biochemical mechanisms are still largely unclear (4-5).

The nucleosome is the basic unit of chromatin and consists of an octamer of histone proteins, including histones H2A, H2B, H3 and H4, which wrap 147 bp of DNA to form the nucleosome core of chromatin. Crystallographic data reveal that the histone octamer is a tripartite structure that consists of a centrally located (H3-H4)₂ tetramer, flanked by two H2A-H2B dimers (6). The core histones are globular except for their N-terminal tails, which undergo many types of post-translational modifications (PTMs), including phosphorylation, methylation, acetylation, ADP-ribosylation, sumoylation, ubiquitination, deimination and proline isomerization (7). Many biochemical and biophysical experiments have identified enzymes that add or remove the modifications in histone residues (8). In addition, chromatin immunoprecipitation assays, coupled with DNA microarray analysis (ChIP-chip) or sequencing (ChIP-Seq) technologies enabled us to glimpse the genomic landscape of individual histone modifications in cells. Although these studies allowed us to correlate the specific histone PTMs to various functional outcomes, the mechanism explaining how histone PTMs can be translated to affect gene expression is still uncertain. Two overlapping models, referred to as 'direct' and 'effector-mediated' models, have been proposed (9). The 'direct' model proposes that histone modifications cause a charge neutralization, which perturbs the interaction between histones and DNA or between different histones in adjacent nucleosomes. This, in turn, affects the higher-order chromatin structure to elicit gene activation. This model merely considers histones as genetic packaging materials and fails to fully explain how certain histone PTMs sometimes contribute to transcriptional suppression. In contrast, the more prevailing 'effector-mediated' model views histones as mediators of biological responses, in which the cues from intracellular signaling cascades affect 'writer'

proteins to modulate histone PTM patterns. These, in turn, serve as the binding platform for 'effector or reader' proteins to recruit or exclude the binding of transcription factors or the interactions of various remodeling proteins to the chromatin, resulting in the initiation of appropriate biological responses.

Numerous studies have demonstrated that UVB activation of intracellular kinase cascades contributes to phosphorylation of transcription factors and the subsequent induction of COX-2 protein expression. A question that still needs to be addressed is whether any epigenetic mechanisms, e.g., DNA methylation or histone PTMs, exist that is responsible for the induction of *cox-2* gene expression after UVB irradiation. This study shows for the first time that histone H3 phosphorylation at Ser10 and Ser28 serves as an important biological platform that translates UVB-mediated MAPK activation into the induction of *cox-2* gene expression in mouse epidermal JB6 cells.

Results

Activation of p38 MAPK and MSK1 plays an important role in UVB-mediated induction of COX-2 and AP-1

Confluent and serum-starved JB6 cells were exposed to UVB (4 kJ/m²) and harvested at different times (0, 1, 2 or 4 h) and disrupted with RIPA buffer. Western blot results show that UVB exposure substantially increased COX-2 and AP-1 (i.e., c-Jun and c-Fos) protein expression in a time-dependent manner. The induction of COX-2 and AP-1 was closely correlated with activation of p38 MAPK and its downstream target kinase, MSK1 (Figure 1A). We have also observed that pretreatment with SB203580 or M89, specific chemical inhibitors of p38 MAPK and MSK1, respectively, suppressed UVB-induced expression of the COX-2 protein (Figure 1B). To confirm whether the p38 MAPK/MSK1 pathway is implicated in UVB-induced COX-2 expression, we exposed JB6 cells, stably transfected with mock (*JB6-mock*) or kinase mutant p38 MAPK plasmids (*JB6-DN-p38 MAPK*), to UVB and examined the expression of UVB-induced COX-2 proteins. Our data show that the induction of UVB-mediated COX-2 protein expression was substantially decreased in *JB6-DN-p38 MAPK* cells, compared with *JB6-mock* cells (Figure 1C). We also observed that UVB-induced COX-2 expression was attenuated in JB6 cells, which were stably transfected with *pCMV5-FLAG-MSK1-A565 COOH-terminal kinase-dead (MSK1-ND)* or with *pCMV5-FLAG-MSK1-A195 NH₂-terminal kinase-dead (MSK1-CD)* plasmids (Figure 1D). Likewise, UVB-induced COX-2 expression was substantially attenuated in JB6 cells that were stably transfected with an *siMSK1* construct, compared with JB6 cells, stably transfected with a scrambled control plasmid (Figure 1E). Together, our data illustrate that p38 MAPK and MSK1 are critical signaling mediators of UVB-induced COX-2 protein expression in JB6 cells.

Phosphorylation of histone H3 at Ser10 and Ser28 by MSK1 mediates UVB-induced COX-2 expression

Next, we attempted to assess global changes in post-translational modifications (PTMs) in histone H3 following UVB irradiation. Confluent and serum-starved JB6 cells were irradiated with UVB and harvested at different times (0, 1, 2 or 4 h). Total histone proteins

were prepared by acid-extraction, followed by trichloroacetic acid (TCA) precipitation. Our results revealed that UVB irradiation strongly induced histone H3 phosphorylation at Ser10 (p-H3S10) and Ser28 (p-H3S28) (Figure 2A). Using a polyclonal antibody that simultaneously recognizes the trimethylated histone H3 at Lys9 and phosphorylated H3 at Ser10 (H3K9me3/p-H3S10), we noticed that the global H3K9me3/p-H3S10 level was also increased. On the other hand, UVB irradiation resulted in a complete disappearance of histone H3 phosphorylation at Thr3 (p-H3T3) and a slight decrease in histone H3 phosphorylation at Thr11 (p-H3T11) (Figure 2A). The functional significance of decreased p-H3T3 and p-H3T11 is unclear at present. In addition, although a number of reports show that histone H3 acetylation at Lys9 (Ac-H3K9) and Lys14 (Ac-H3K14) is closely coupled with histone phosphorylation during mitogenic or hormonal stimulation in mammalian cells (10-11), we did not observe such changes (Figure 2A).

Because phosphorylation of histone H3 at Ser10 and Ser28 was the only inducible post-translational modification occurring in histone H3 after UVB irradiation, we examined the possible role of these phosphorylations in the UVB-induction of the COX-2 protein. To address this issue, JB6 cells, stably overexpressing FLAG-H3.3 (JB6-FLAG-H3.3), FLAG-H3.3-S10A (JB6-FLAG-H3.3-S10A), FLAG-H3.3-S28A (JB6-FLAG-H3.3-S28A), or *FLAG-H3.3-S10/28A* (JB6-FLAG-H3.3-S10/28A) were generated by transient transfection, followed by G148 selection for 2 weeks. Established stable JB6 cells were then co-transfected with the *cox-2* luciferase reporter plasmid and the β -galactosidase plasmid. The resulting luciferase activity was measured and activity normalized with β -galactosidase activity after UVB exposure. The results show that no discernable differences in luciferase activity among the established stable JB6 cells were observed in the absence of UVB. However, we observed that the level of UVB-induced COX-2 luciferase activation was significantly attenuated in mutant *JB6-FLAG-H3.3-S10A* and *JB6-FLAG-H3.3-S28A* cells, compared with *JB6-FLAG-H3.3* cells at 24 h post-UVB irradiation (Figure 2B). In addition, the degree of UVB-induced COX-2 luciferase activation in *JB6-FLAG-H3.3-S10/28A* cells was lower than in either *JB6-FLAG-H3.3-S10A* or *JB6-FLAG-H3.3-S28A* cells (Figure 2B). In order to examine whether phosphorylation of histone H3 at Ser10 and Ser28 is indeed responsible for UVB-induced COX-2 and AP-1 protein expression, JB6 stable cells (*JB6-FLAG-H3.3*, *JB6-FLAG-H3.3-S10A*, *JB6-FLAG-H3.3-S28A*, and *JB6-FLAG-H3.3-S10/28A*) were exposed to UVB and harvested at different times (0, 1, 2, or 4 h) and cell lysates were collected for Western blot analysis. Our results show that UVB-induced protein expression of COX-2 and AP-1 (i.e., c-Jun and c-Fos) was attenuated in *JB6-FLAG-H3.3-S10A* or *JB6-FLAG-H3.3-S28A* cells, compared with *JB6-FLAG-H3.3* cells (Figure 2C). We also observed that UVB-induced COX-2 and AP-1 protein expression was barely detectable in *JB6-FLAG-H3.3-S10/28A* cells. Unlike COX-2 and AP-1 proteins, we found that the protein expression of CREB and β -actin was unaffected, suggesting that histone H3 phosphorylation at Ser10 and Ser28 might cooperate to control UVB-inducible COX-2 and AP-1 protein expression (Figure 2C).

The finding that histone H3 phosphorylation at Ser10 and Ser28 was crucial in UVB-induced COX-2 and AP-1 protein expression led us to examine whether the UVB-activated p38 MAPK/MSK1 pathway might be responsible for histone H3 phosphorylation at Ser10

and Ser28. Our data reveal that pretreatment of cells with SB203580 or H89 substantially decreased UVB-induced histone H3 phosphorylation at Ser10 (p-H3S10) and Ser28 (p-H3S28) (Figure 3A). In addition, unlike JB6 cells stably transfected with mock plasmid, UVB-induced histone H3 phosphorylation at Ser10 and Ser28 was notably suppressed in *JB6-DN-p38 MAPK* cells (Figure 3B). In order to examine whether MSK1 is implicated in UVB-induced histone H3 phosphorylation at Ser10 and Ser28, we have generated two independent JB6 cell types, whose endogenous MSK1 expression was silenced by two independent lentiviral *shRNA* constructs (Figure 3C). As a result, we found that silencing MSK1 attenuated UVB-induced histone H3 phosphorylation at Ser10 and Ser28. Collectively, these data illustrate that the p38 MAPK/MSK1 pathway plays a critical role in UVB-induced histone H3 phosphorylation at Ser10 and Ser28 in JB6 cells.

UVB activation has no effect on histone H3 trimethylation levels

Histone H3 methylation specifically occurs at the Lys4, 9, 27, 36 and 79 residues and the ϵ -amino group of each histone lysine residue can accept up to three methyl groups. With a few exceptions, trimethylation of H3K9 and H3K27 is associated with transcriptional repression, whereas trimethylation of H3K4, H3K36 and H3K79 is associated with transcriptional activation (12). H3K9 and H3K27 are located in adjacent residues of H3S10 and H3S28. An antagonistic interaction is believed to exist between H3K9 trimethylation and H3S10 phosphorylation or between H3K27 trimethylation and H3S28 phosphorylation (13-14). Thus, we next decided to examine whether global histone H3 trimethylation levels are changed after UVB irradiation. Our results show that UVB does not affect the global trimethylation levels of histone H3 at Lys4 (H3K4me3), Lys9 (H3K9me3) and Lys27 (H3K27me3) (Figure 4A). The protein expression of G9a, euchromatic H3K9 methyltransferase or that of Ezh2, Eed, Suz12, and RbAP48, all of which are the components of protein repressive complex-2 (PRC2) that catalyzes H3K27 methylation, was also unaffected (Figure 4B). In a previous study, Hung and colleagues (15) reported that direct phosphorylation of Ezh2 by Akt1 at Ser21 is responsible for suppressing methyltransferase activity. Although Akt and its downstream kinase, S6K1, are strongly activated by UVB (Figure 4C) in our experiments, we did not detect phosphorylation of Ezh2 (Figure 4B).

We next examined the possibility that UVB affects H3K9 and H3K27 methylation effector proteins. HP-1 proteins are classified into three isotopes that include HP1 α , HP1 β and HP1 γ . While HP1 α and HP1 β predominantly exist in the heterochromatin, HP1 γ can be found in the euchromatin. Western blot analysis revealed that UVB irradiation did not affect the protein expression of HP1 α , HP1 β or HP1 γ (Figure 4D). However, we found that UVB caused an increased phosphorylation of HP1 γ at Ser83 (Figure 4D). Although protein kinase A (PKA) is reported to induce phosphorylation of HP1 γ at Ser83 and antagonize the suppressive effect of HP1 γ (16), we did not detect PKA phosphorylation, suggesting that kinase(s) other than PKA might be responsible for HP1 γ phosphorylation induced by UVB. In addition, we found that UVB did not affect the expression of other chromobox proteins such as Cbx2 and Cbx4 (Figure 4E), which are presumed to bind to H3K27me3 and mediate the gene suppressive effects of H3K27me3 (17). Cbx7 expression was also not detectable in

our experimental system. Based on these results, we presume that histone H3 trimethylation might play a minimal role in UVB-induced COX-2 expression.

14-3-3 protein isoforms selectively bind to UVB-induced phosphorylated histone H3 *in vitro* and silencing 14-3-3 ϵ attenuates UVB-induced COX-2 expression

14-3-3 proteins are ubiquitously expressed and control a variety of cellular processes, such as cell cycle checkpoint, MAPK activation, apoptosis and transcriptional regulation. Seven 14-3-3 isotype proteins (β , γ , ϵ , η , σ , τ , ζ) exist in mammalian cells and a large amount of sequence identity and conservation exists between isoforms (18). In fact, Mahadevan and colleagues showed that selected 14-3-3 protein isotypes (γ , ϵ and ζ) bind to phosphorylated histone H3 at Ser10 (19). The possible recognition of 14-3-3 proteins of phosphorylated H3S28 was also revealed by phospho-H3 peptide pull-down assay (20).

However, to our knowledge, no experimental attempts have been made to identify the 14-3-3 protein isotypes that recognize endogenously phosphorylated histone H3. To address this issue, confluent and serum-starved JB6 cells were or were not exposed to UVB irradiation and then harvested after 1 h. Total histone proteins were isolated by acid extraction, followed by TCA precipitation. Extracted histone proteins were then subjected to pull-down assays with individual recombinant human GST-conjugated 14-3-3 isoform proteins. As a result, we observed that all recombinant GST-14-3-3 isoform proteins extracted from UVB-irradiated JB6 cells bound to total histone H3 (Figure 5A). In addition, Western blot analysis revealed that phosphorylated histone H3S10 and H3S28 bands were detected from selected GST-14-3-3 protein pull-down lysates (β , γ , ϵ , η , τ for p-H3S10 and β , γ , ϵ , τ for p-H3S28) (Figure 5B). On the other hand, none of the 14-3-3 protein isoforms bound to UVB-induced phosphorylated c-Jun or p65 (Figure 5B). Notably, we found that UVB irradiation had no effect on the basal level of 14-3-3 protein isoforms (β , γ , ϵ , η , or τ) (Figure 5C).

The carboxy-terminal domain (CTD) of the largest subunit of RNA polymerase II consists of multiple tandem conserved heptapeptide repeats (e.g., YSPTSPS, with up to 52 repeats in mammals). This unusual structure serves as a docking platform for factors involved in various co-transcriptional events and phosphorylation of heptapeptide repeats at Ser2 and/or Ser5 by Cdk8, Cdk9 or ERK1/2 defines the transcriptional activation status of RNA polymerase II (21). Using pull-down lysates of the recombinant GST-14-3-3 isoform protein, we observed a strong interaction between 14-3-3 ϵ and Cdk9 (Figure 5D), a subunit of the post-transcriptional elongation factor b (P-TEFb) that activates transcriptional elongation and RNA processing (22). Using human breast epithelial MCF10A cells stably infected with HA-14-3-3 ϵ , we found that the 14-3-3 ϵ protein can interact with total histone H3 and Cdk9 proteins after UVB irradiation. In order to determine whether 14-3-3 ϵ is implicated in UVB-induced COX-2 and AP-1 expression, we generated JB6 cells in which 14-3-3 ϵ was selectively silenced by lentiviral transduction. Our results show that UVB-induced COX-2 and c-Jun protein expression was substantially attenuated when 14-3-3 ϵ was silenced (Figure 5E). Collectively, our studies show that UVB-induced histone H3 phosphorylation at Ser10 and Ser28 is mediated by activation of p38 MAPK and MSK1 and that 14-3-3 ϵ is a critical mediator of UVB-induced COX-2 and AP-1 protein expression by

recognizing histone phosphorylation marks at Ser10 and Ser28 and recruiting Cdk9 and facilitating RNA polymerase II phosphorylation in the chromatin (Figure 5G).

Discussion

Previous studies indicated that phosphorylation of transcription factors by p38 MAPK/MSK1 kinase activation is responsible for UVB-inducible *cox-2* gene expression (23). In the current study, we present another mechanism of action that is responsible for UVB-induced COX-2 expression associated with histone H3 phosphorylation at Ser10 and Ser28. Both histone phosphorylation at Ser10 and Ser28 appear to contribute equally to UVB-induced COX-2 expression. This is based on the observation that stable expression of the *FLAG-H3S10A* or *FLAG-H3S28A* construct in JB6 cells attenuated UVB-induced COX-2 expression to a similar degree and, importantly, UVB-induced COX-2 expression was completely abolished in JB6 cells that were stably transfected with *FLAG-H3S10/28A* (Figure 2C). Suppression of UVB-induced COX-2 expression in JB6 cells, stably transfected with mutant plasmids, could be attributed to the suppressive expression of c-Jun and c-Fos proteins, because these proteins exhibited a similar expression pattern with COX-2 in the same set of experiments. However, based on the observations that 14-3-3 proteins could bind to phosphorylated histone H3, but not phosphorylated c-Jun or c-Fos proteins (Figure 5B) and silencing of the 14-3-3 ϵ protein suppressed UVB-induced COX-2 expression in JB6 cells (Figure 5E), we presume that histone H3 phosphorylation at Ser10 and Ser28 can control UVB-induced COX-2 expression by routes other than affecting c-Jun and c-Fos expression.

The phosphorylated H3S10 mark is related to two opposite states of chromatin, including heterochromatin during mitosis and euchromatin during interphase (24). In fact, histone H3 phosphorylation at Ser10 is a well-known marker that represents the mitotic state and a strong correlation with chromosome condensation has been observed (25). Likewise, histone H3 phosphorylation at Ser28 also occurs during mitosis and localization of aurora B kinase, a putative mitotic histone H3 kinase, coincides with histone H3 phosphorylation at Ser10 and Ser28 during early mitosis (26). On the other hand, histone H3 phosphorylation at Ser10 during interphase was reported to occur in a much smaller euchromatic fraction and correlate with transcriptional activation of immediate early response genes (IEGs), such as *c-jun* and *c-fos* (27). While aurora kinase B might be the only mitotic kinase responsible for H3S10 phosphorylation and, possibly, H3S28 phosphorylation (28), a variety of kinases are presumed to phosphorylate histone H3 at Ser10 and/or Ser28 during interphase (29). Why such a large number of kinases are required to phosphorylate much smaller euchromatic fractions and how the activities of individual kinases are orchestrated in cells are unclear at present. We speculate that a refined coordination of multiple kinases is possibly required to exert appropriate biological responses, depending on the intracellular contexts or in response to a host of diverse extracellular stimuli. In addition, we believe that searching for compounds that would interfere with the interaction between 14-3-3 proteins with the p-H3S10 and p-H3S28 marks might serve as a novel and more effective strategy to suppress *cox-2* gene expression and, eventually, inflammation rather than developing those chemicals that suppress the activities of individual kinases, which are reported to contribute to *cox-2* gene expression.

Unlike histone phosphorylation or acetylation, histone methylation has been regarded as a stable mark (30). Supporting this hypothesis, we observed that H3K4me3, H3K9me3 and H3K27me3 levels were unaffected after UVB irradiation in JB6 cells (Figure 4A). However, Allis and colleagues (8) have proposed the binary-switch model that accounts for the possible antagonistic relationships between histone methylation and phosphorylation. For example, histone H3 phosphorylation at Ser10 and Ser28 might affect the protein binding of H3K9 and H3K27 effector proteins (31). While this hypothesis was examined using peptide pull-down assays and therefore awaits further experimental verifications *in vivo*, we observed that UVB irradiation caused HP1 γ phosphorylation at Ser83 (Figure 4D), which is an effector protein of the H3K9 methylation mark. Although the functional significance of this phosphorylation in UVB-induced COX-2 expression is unclear at present, Lombark *et al.* previously reported that HP1 γ phosphorylation contributes to its binding to the Ku70 protein and phosphorylation of the RNA polymerase II protein at Ser5 (16). If this observation is true, we can assume that, in addition to its roles in reading methyl-marks of histone H3, HP1 γ might actively participate in UVB-mediated gene expression or DNA damage responses by recruiting chromatin-related proteins, including Ku70, which, in turn, affects and creates the chromatin environment to promote *cox-2* gene expression in response to UVB. Therefore, to examine in the future whether HP1 γ phosphorylation indeed affects *cox-2* gene expression after UVB irradiation would be interesting as would the identification of proteins that are recruited to and/or occluded from the *cox-2* promoter when the HP1 γ protein is phosphorylated.

Materials and Methods

Cell culture and chemicals

JB6 mouse epidermal skin cells were cultured in modified Eagle's medium (MEM) with 5% fetal bovine serum (FBS). Human mammary epithelial MCF10A cells were grown in Dulbecco's modified Eagle's medium-F12 (DMEM/F12) (Invitrogen, Carlsbad, CA), supplemented with 5% horse serum (Invitrogen), 1% penicillin-streptomycin (Invitrogen), 0.5 μ g/ml hydrocortisone (Sigma, St. Louis, MO), 100 ng/ml cholera toxin (Sigma), 10 μ g/ml insulin (Sigma), and 20 ng/ml recombinant human EGF (Peprotech, Rocky Hill, NJ). Before the experiments, confluent JB6 or MCF10A cells were rendered quiescent by starvation in serum-free MEM and analyzed immediately or stimulated by UVB for an additional time period. When required, cells were pretreated with SB203580 (Calbiochem, La Jolla, CA) or H89 (Calbiochem) for 1 h. The process for establishing JB6-mock, JB6-siMock, JB6-DN-p38 MAPK, JB6-siMSK1, JB6-MSK1-WT, JB6-MSK1-ND, and JB6-MSK1-CD cells has been previously described (32). JB6 stable cells overexpressing FLAG-H3.3 constructs were generated by transient transfection with pcDNA3.1-FLAG, pcDNA3.1-FLAG-H3.3, pcDNA3.1-FLAG-H3.3S10A, pcDNA3.1-FLAG-H3.3S28A and *pcDNA3.1-FLAG-H3.3S10/28A* plasmids, followed by 400 μ g/ml G418 selection (Invitrogen) for 2 wk.

Generation of stable cells by retroviral and lentiviral transduction

Stable gene knockdown JB6 cell lines were established by lentiviral transduction. In brief, 293T packaging cells were co-transfected with 3 μ g lentiviral shRNA constructs together

with an equal amount of lentiviral helper vectors (*pMD.2G* and *pCMV-VSVG*), using the JetPEI reagent (Qbiogene, Carlsbad, CA). Media for 293T cells was replaced after 24 h with MEM/0.5% FBS and incubated for another 24-48 h. The viral supernatant fraction was collected and filtered using a 0.45 μm syringe filter. JB6 cells were infected with 10 μl of the viral supernatant fraction, supplemented with 5% FBS and 10 $\mu\text{g}/\text{mL}$ polybrene for 12 h at 37 $^{\circ}\text{C}$, and further selected with 4 $\mu\text{g}/\text{ml}$ puromycin (Calbiochem) for 2 days. Multiple sets of *pLKO.1* vector-based shRNA constructs were acquired from the University of Minnesota RNAi Core Facility (Minneapolis, MN) and gene knockdown efficiency of individual viral constructs was evaluated by Western blotting.

Stable MCF10A cells overexpressing HA-14-3-3 constructs were established by retroviral transduction. Packaging cells (293T) were co-transfected with *pBabe-HA-14-3-3* isoforms and retroviral helper vectors (*pCG-GPG* and *pCG-VSVG*). Viral supernatant fractions were collected and filtered with a 0.45 μm syringe filter. MCF10A cells were transduced with the viral supernatant fraction, supplemented with 5% FBS and 10 $\mu\text{g}/\text{mL}$ polybrene for 12 h at 37 $^{\circ}\text{C}$, and further selected with 4 $\mu\text{g}/\text{ml}$ puromycin (Calbiochem) for 2 days.

Plasmids and antibodies

Lentiviral helper plasmids (*pMD.2G* and *pCMV-VSVG*) were acquired from Addgene (Boston, MA). Retroviral helper vectors (*pCG-GPG* and *pCG-VSVG*) were kind gifts from Dr. Gordon Peters (Cancer Research UK, London, UK). Seven *pGEX-14-3-3* isoform (β , γ , ϵ , η , σ , τ , ζ) constructs were kindly provided by Dr. Cheryl Walker (University of Texas M.D. Anderson Cancer Center (Smithville, TX)). The 14-3-3 isoform cDNAs were digested and subcloned into the *pBabe-HA-puro* vector. Site-directed mutagenesis of all plasmids was conducted using the QuikChange Site-Directed Mutagenesis Kit (Stratagene, La Jolla, CA). The antibody to detect total COX-2 was purchased from Cayman Chemical Inc. (Ann Arbor, MI). Anti-FLAG and mouse monoclonal β -actin antibodies were purchased from Sigma (St. Louis, MO). Cdk9 antibodies were purchased from Abcam (Cambridge, MA). Micrococcal nuclease and antibodies to detect c-Jun, c-Fos, p38 MAPK, phosphorylated p38 MAPK, phosphorylated MSK1, HP1 α , HP1 β , HP1 γ , G9a, Ezh2, Suz12, and 14-3-3 isoforms (β , γ , ϵ , η , τ) were purchased from Cell Signaling Technology (Beverly, MA). Total MSK1 and total GST antibodies were purchased from Santa Cruz Biotechnology (Santa Cruz, CA). Antibodies to detect H3K4me3, H3K9me3, H3K27me3, phosphorylated H3 (Ser10), phosphorylated H3 (Ser28), and Eed were purchased from Millipore Corporation (Billerica, MA). The antibody to detect phosphorylation of Ezh2 (Ser21) was purchased from Bethyl Laboratories Inc. (Montgomery, TX).

Isolation of histones and Western blotting

Cultured cells were collected and washed twice with ice-cold 1 \times phosphate-buffered saline (PBS). After centrifugation at 12,000 rpm for 5 min, cells were resuspended with 200 μl RIPA buffer (50 mM Tris-HCl at pH 8.0, 150 mM NaCl, 1% NP-40, 0.5% DOC, 0.1% SDS, 1 mM Na_3VO_4 , 1 mM DTT, 1 mM PMSF) or with 200 μl 1% SDS lysis buffer (1% SDS in Tris-EDTA buffer, pH 8.0) and kept on ice for 30 min. After lysates were collected in 1% SDS lysis buffer, they were heavily sonicated on ice to disrupt genomic DNA. Cell lysates were prepared in 1 \times RIPA buffer and used for measuring the expression or phosphorylation

status of soluble kinases and transcription factors. Cell lysates were prepared in 1% SDS lysis buffer and used for measuring the expression or phosphorylation status of insoluble chromatin-bound proteins. For isolation of histone proteins, cells were resuspended in 180 μ l of 1 \times PBS and 20 μ l of 2 N HCl (final concentration of 0.2 N HCl) and incubated on ice for 30 min. The lysate was centrifuged at 12,000 rpm for 5 min at 4 $^{\circ}$ C and the supernatant fraction was collected. The supernatant fraction was then mixed with 100 μ l 50% TCA and kept on ice for 30 min. The precipitated proteins were collected by centrifugation at 12,000 rpm for 5 min at 4 $^{\circ}$ C, washed twice with acetone and dissolved in H₂O. The protein concentration was measured using the Pierce BCA Protein Assay Kit (Thermo Fisher Scientific Inc., Waltham, MA). Cell lysate (30 μ g) or 1 μ g histone acid extract was resolved by SDS-PAGE and transferred onto PVDF membranes (Millipore, Danvers, MA). The membranes were incubated in blocking buffer (5% milk/1 \times PBST) and hybridized with the appropriate primary antibodies in 1 \times PBS solution containing 3% BSA overnight at 4 $^{\circ}$ C. After washing 3 times with 1 \times PBST (1 \times PBS with 0.1% Tween-20 solution) for 30 min, the membrane was hybridized with a horseradish peroxidase (HRP)-conjugated secondary antibody (Santa Cruz Biotechnology, Santa Cruz, CA) for 1 h at room temperature and washed 3 times with 1 \times PBST solution for 30 min. The membrane was visualized by using the enhanced chemiluminescence (ECL) detection system.

GST pull-down assay and immunoprecipitation

GST-fused recombinant 14-3-3 isoform proteins were purified on glutathione-Sepharose beads (GE Healthcare, Piscataway, NJ) and dialyzed. In order to examine the interaction between 14-3-3 proteins and histones or other transcription factors, 1 μ g of each recombinant GST-14-3-3 isoform protein was mixed with 15 μ g of histone acid-extracts and incubated overnight at 4 $^{\circ}$ C. Recombinant GST-14-3-3 isoform proteins were immunoprecipitated with glutathione-Sepharose beads and the bound proteins were washed 3 times with 1 \times PBS and denatured in 1 \times sample buffer. The interaction of proteins with GST-fusion proteins was assessed by Western blotting. The interaction of 14-3-3 ϵ with total histone H3 or Cdk9 in MCF10A cells was examined by immunoprecipitation, followed by Western blot analysis. More specifically, MCF10A cells were retrovirally infected with the *pBabe-puro-HA-14-3-3 ϵ* construct. After puromycin selection for 2 days, MCF10A cells were harvested and disrupted with RIPA buffer containing micrococcal nuclease (100 unit/ml) for 30 min on ice. After immunoprecipitation with HA-resin (Sigma, St. Louis, MA), the interaction of HA-14-3-3 ϵ protein with cellular histone H3 and Cdk9 was examined by Western blot analysis.

Acknowledgements

This work was supported by The Hormel Foundation and National Institutes of Health grants CA120388, R37 CA081064, ES016548 and Grant No. R31-2008-000-10103-0 from the Korea WCU project of the MEST and the NRF.

References

1. Wang D, Dubois RN. The role of COX-2 in intestinal inflammation and colorectal cancer. *Oncogene*. 2009 Epub 2009/12/01.

2. Rundhaug JE, Mikulec C, Pavone A, Fischer SM. A role for cyclooxygenase-2 in ultraviolet light-induced skin carcinogenesis. *Mol Carcinog.* 2007; 46(8):692–8. Epub 2007/04/20. [PubMed: 17443745]
3. Rundhaug JE, Fischer SM. Cyclo-oxygenase-2 plays a critical role in UV-induced skin carcinogenesis. *Photochem Photobiol.* 2008; 84(2):322–9. Epub 2008/01/16. [PubMed: 18194346]
4. Fernau NS, Fugmann D, Leyendecker M, Reimann K, Grether-Beck S, Galban S, et al. Role of HuR and p38MAPK in ultraviolet B-induced post-transcriptional regulation of COX-2 expression in the human keratinocyte cell line HaCaT. *J Biol Chem.* 2010; 285(6):3896–904. Epub 2009/11/18. [PubMed: 19917608]
5. Zhang J, Bowden GT. UVB irradiation regulates Cox-2 mRNA stability through AMPK and HuR in human keratinocytes. *Mol Carcinog.* 2008; 47(12):974–83. Epub 2008/05/02. [PubMed: 18449856]
6. Luger K, Mader AW, Richmond RK, Sargent DF, Richmond TJ. Crystal structure of the nucleosome core particle at 2.8 Å resolution. *Nature.* 1997; 389(6648):251–60. Epub 1997/09/26. [PubMed: 9305837]
7. Strahl BD, Allis CD. The language of covalent histone modifications. *Nature.* 2000; 403(6765):41–5. Epub 2000/01/19. [PubMed: 10638745]
8. Allis CD, Berger SL, Cote J, Dent S, Jenuwien T, Kouzarides T, et al. New nomenclature for chromatin-modifying enzymes. *Cell.* 2007; 131(4):633–6. Epub 2007/11/21. [PubMed: 18022353]
9. Kouzarides T. Chromatin modifications and their function. *Cell.* 2007; 128(4):693–705. Epub 2007/02/27. [PubMed: 17320507]
10. Cheung P, Tanner KG, Cheung WL, Sassone-Corsi P, Denu JM, Allis CD. Synergistic coupling of histone H3 phosphorylation and acetylation in response to epidermal growth factor stimulation. *Mol Cell.* 2000; 5(6):905–15. Epub 2000/07/27. [PubMed: 10911985]
11. Lo WS, Trievel RC, Rojas JR, Duggan L, Hsu JY, Allis CD, et al. Phosphorylation of serine 10 in histone H3 is functionally linked in vitro and in vivo to Gcn5-mediated acetylation at lysine 14. *Mol Cell.* 2000; 5(6):917–26. Epub 2000/07/27. [PubMed: 10911986]
12. Wang GG, Allis CD, Chi P. Chromatin remodeling and cancer, Part I: Covalent histone modifications. *Trends Mol Med.* 2007; 13(9):363–72. Epub 2007/09/08. [PubMed: 17822958]
13. Fischle W, Tseng BS, Dormann HL, Ueberheide BM, Garcia BA, Shabanowitz J, et al. Regulation of HP1-chromatin binding by histone H3 methylation and phosphorylation. *Nature.* 2005; 438(7071):1116–22. Epub 2005/10/14. [PubMed: 16222246]
14. Hirota T, Lipp JJ, Toh BH, Peters JM. Histone H3 serine 10 phosphorylation by Aurora B causes HP1 dissociation from heterochromatin. *Nature.* 2005; 438(7071):1176–80. Epub 2005/10/14. [PubMed: 16222244]
15. Cha TL, Zhou BP, Xia W, Wu Y, Yang CC, Chen CT, et al. Akt-mediated phosphorylation of EZH2 suppresses methylation of lysine 27 in histone H3. *Science.* 2005; 310(5746):306–10. [PubMed: 16224021]
16. Lomberk G, Bensi D, Fernandez-Zapico ME, Urrutia R. Evidence for the existence of an HP1-mediated subcode within the histone code. *Nat Cell Biol.* 2006; 8(4):407–15. Epub 2006/03/15. [PubMed: 16531993]
17. Bernstein E, Duncan EM, Masui O, Gil J, Heard E, Allis CD. Mouse polycomb proteins bind differentially to methylated histone H3 and RNA and are enriched in facultative heterochromatin. *Mol Cell Biol.* 2006; 26(7):2560–9. Epub 2006/03/16. [PubMed: 16537902]
18. Yaffe MB. How do 14-3-3 proteins work?-- Gatekeeper phosphorylation and the molecular anvil hypothesis. *FEBS Lett.* 2002; 513(1):53–7. Epub 2002/03/26. [PubMed: 11911880]
19. Macdonald N, Welburn JP, Noble ME, Nguyen A, Yaffe MB, Clynes D, et al. Molecular basis for the recognition of phosphorylated and phosphoacetylated histone h3 by 14-3-3. *Mol Cell.* 2005; 20(2):199–211. Epub 2005/10/26. [PubMed: 16246723]
20. Winter S, Fischle W, Seiser C. Modulation of 14-3-3 interaction with phosphorylated histone H3 by combinatorial modification patterns. *Cell Cycle.* 2008; 7(10):1336–42. Epub 2008/04/18. [PubMed: 18418070]
21. Eglhoff S, Murphy S. Cracking the RNA polymerase II CTD code. *Trends Genet.* 2008; 24(6):280–8. Epub 2008/05/07. [PubMed: 18457900]

22. Buratowski S. Progression through the RNA polymerase II CTD cycle. *Mol Cell*. 2009; 36(4):541–6. Epub 2009/11/28. [PubMed: 19941815]
23. Bachelor MA, Cooper SJ, Sikorski ET, Bowden GT. Inhibition of p38 mitogen-activated protein kinase and phosphatidylinositol 3-kinase decreases UVB-induced activator protein-1 and cyclooxygenase-2 in a SKH-1 hairless mouse model. *Mol Cancer Res*. 2005; 3(2):90–9. Epub 2005/03/10. [PubMed: 15755875]
24. Perez-Cadahia B, Drobic B, Davie JR. H3 phosphorylation: dual role in mitosis and interphase. *Biochem Cell Biol*. 2009; 87(5):695–709. Epub 2009/11/10. [PubMed: 19898522]
25. Johansen KM, Johansen J. Regulation of chromatin structure by histone H3S10 phosphorylation. *Chromosome Res*. 2006; 14(4):393–404. Epub 2006/07/06. [PubMed: 16821135]
26. Goto H, Yasui Y, Nigg EA, Inagaki M. Aurora-B phosphorylates Histone H3 at serine28 with regard to the mitotic chromosome condensation. *Genes Cells*. 2002; 7(1):11–7. Epub 2002/02/22. [PubMed: 11856369]
27. Nowak SJ, Corces VG. Phosphorylation of histone H3: a balancing act between chromosome condensation and transcriptional activation. *Trends Genet*. 2004; 20(4):214–20. Epub 2004/03/26. [PubMed: 15041176]
28. Prigent C, Dimitrov S. Phosphorylation of serine 10 in histone H3, what for? *J Cell Sci*. 2003; 116(Pt 18):3677–85. Epub 2003/08/15. [PubMed: 12917355]
29. Bode AM, Dong Z. Inducible covalent posttranslational modification of histone H3. *Sci STKE*. 2005; 2005(281):re4. Epub 2005/04/28. [PubMed: 15855410]
30. Shilatifard A. Chromatin modifications by methylation and ubiquitination: implications in the regulation of gene expression. *Annu Rev Biochem*. 2006; 75:243–69. Epub 2006/06/08. [PubMed: 16756492]
31. Fischle W, Wang Y, Allis CD. Binary switches and modification cassettes in histone biology and beyond. *Nature*. 2003; 425(6957):475–9. Epub 2003/10/03. [PubMed: 14523437]
32. Zhang Y, Dong Z, Nomura M, Zhong S, Chen N, Bode AM. Signal transduction pathways involved in phosphorylation and activation of p70S6K following exposure to UVA irradiation. *J Biol Chem*. 2001; 276(24):20913–23. Epub 2001/03/30. [PubMed: 11279232]

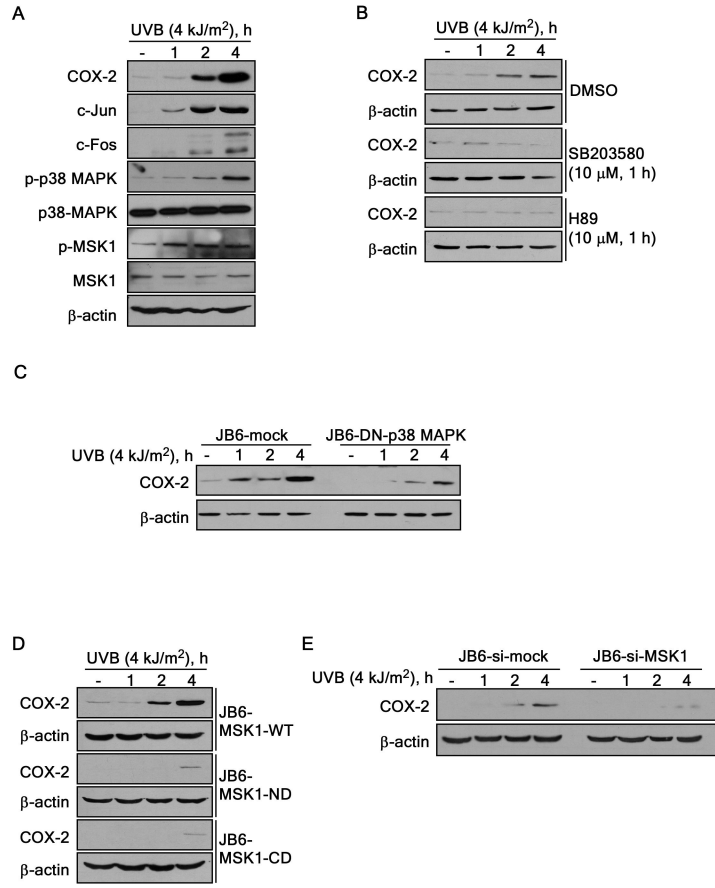


Figure 1. UVB-induced COX-2 expression corresponds with activation of p38 MAPK and MSK1 in JB6 cells. (A) UVB irradiation induces COX-2 and AP-1 protein expression and activation of p38 MAPK and MSK1. (B) Pretreatment of cells with SB203580, a p38 MAPK chemical inhibitor, or H89, a MSK1 chemical inhibitor, suppresses UVB-induced COX-2 expression. (C) UVB-mediated induction of COX-2 is attenuated in JB6-DN-p38MAPK cells, compared with JB6-mock cells. (D) UVB-induced COX-2 expression is substantially suppressed in JB6-MSK1-ND or in JB6-MSK1-CD cells, compared with JB6-MSK1-WT cells (E) UVB-induced COX-2 expression is attenuated in JB6-si-MSK1 cells, compared with JB6-si-mock cells.

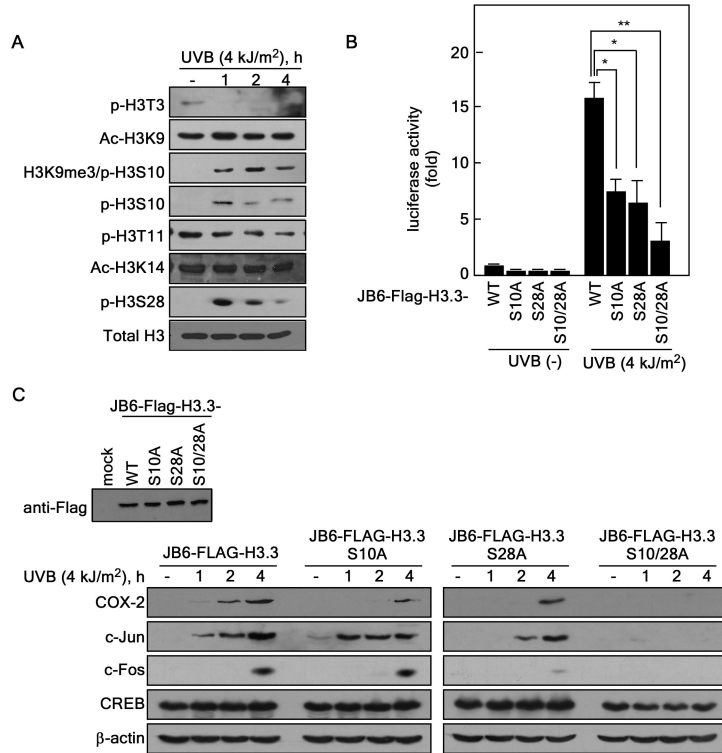
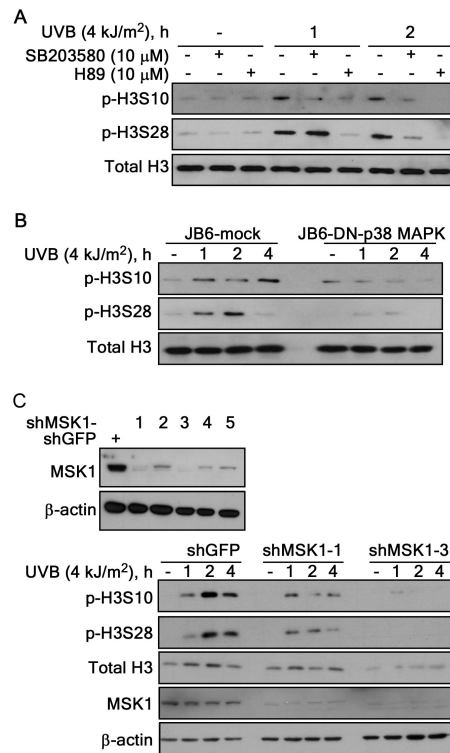


Figure 2.

UVB-induced COX-2 expression requires phosphorylation of histone H3 at Ser10 and Ser28 in JB6 cells. (A) UVB affects several histone H3 phosphorylation marks. Changes in post-translational modification of total histone H3 were examined by Western blot, using acid-extracted histones. (B) UVB-induced COX-2 luciferase activation is significantly attenuated in JB6 cells stably transfected with FLAG-H3.3 Ser10 and/or Ser28 mutants, compared with JB6-FLAG-H3.3-WT cells. JB6 cells, stably transfected with FLAG-H3.3-WT, S10A, S28A and S10/28A, were transiently transfected with 1 μ g *COX-2 luciferase* promoter and 1 μ g β -galactosidase. At 48 h post-transfection, cells were treated or not treated with UVB (4 kJ/m²) irradiation and harvested and the lysates were measured for COX-2 luciferase activity. Data are shown as means \pm S.D. and asterisks (*, $p < 0.05$; **, $p < 0.01$) indicate a significant decrease compared to wildtype cells. (C) JB6 cells that were stably transfected with FLAG-H3.3-WT, -S10A, -S28A or -S10/28A were irradiated with UVB (4 kJ/m²) and collected at different time points (0, 1, 2, or 4 h) and the lysates were used for Western blot assay.

**Figure 3.**

p38 MAPK and MSK1 are involved in UVB-induced histone H3 phosphorylation at Ser10 and Ser28 in JB6 cells. (A) Pretreatment of JB6 cells with SB203580 or H89 suppresses UVB-induced histone H3 phosphorylation at Ser10 and Ser28. JB6 cells were treated with SB203580 for 1 h prior to UVB irradiation (4 kJ/m²). After UVB irradiation, cells were collected at different times (0, 1, and 2 h) and changes in histone H3 phosphorylation at Ser10 and Ser28 were measured by Western blot. (B) JB6-mock and JB6-DN-p38MAPK cells were irradiated with UVB (4 kJ/m²), harvested at different times (0, 1, 2, 4 h). Changes in histone H3 phosphorylation at Ser10 and Ser28 were measured by Western blot. (C) JB6 cells were transduced with 5 different kinds of lentiviral vectors. Two independent JB6 cell clones, in which endogenous MSK1 was completely lost, were chosen for evaluating the effects of UVB-induced histone H3 phosphorylation at Ser10 and Ser28.

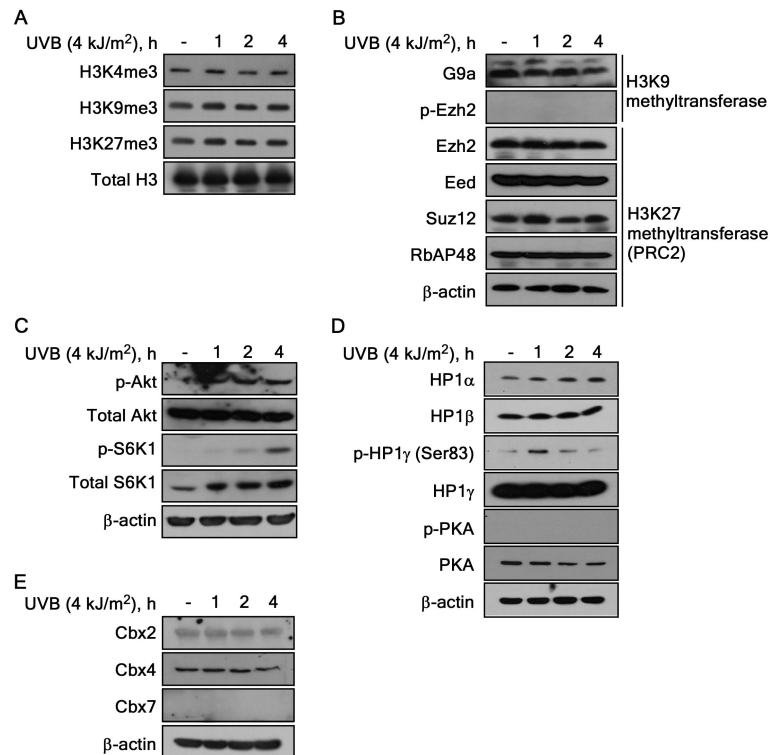
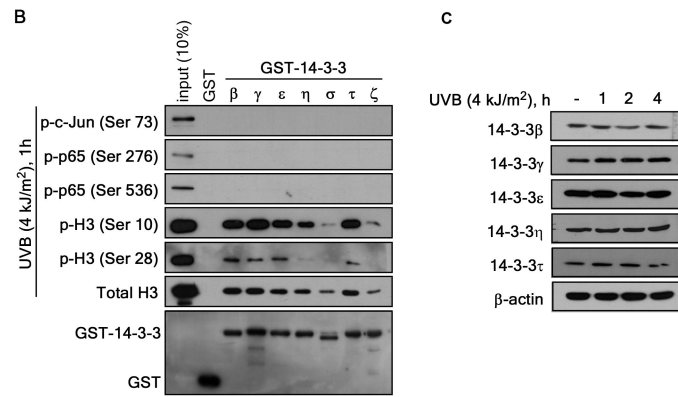
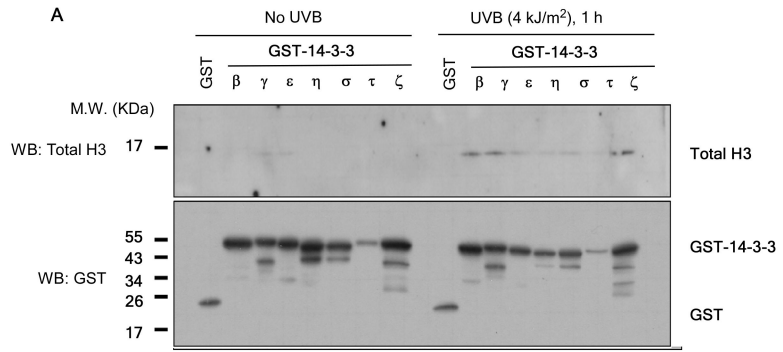


Figure 4.

UVB irradiation has no effect on the methylation status of histone H3 in JB6 cells. (A) JB6 cells were irradiated with UVB (4 kJ/m²) and harvested at different times (0, 1, 2, and 4 h) and the global changes in histone trimethylation at Lys4, Lys9 and Lys27 were measured by Western blot, using total histone extracts. (B) JB6 cells were irradiated with UVB and harvested at different times. Cells were disrupted in RIPA buffer. Western blot analysis was conducted to measure the changes in the expression of various histone H3 methyltransferases, (C) phosphorylation changes of Akt and S6K1, (D) the expression of HP1 protein isoforms as well as HP1γ phosphorylation at Ser83, and (E) the expression of chromobox (Cbx) proteins were measured by Western blot analysis.



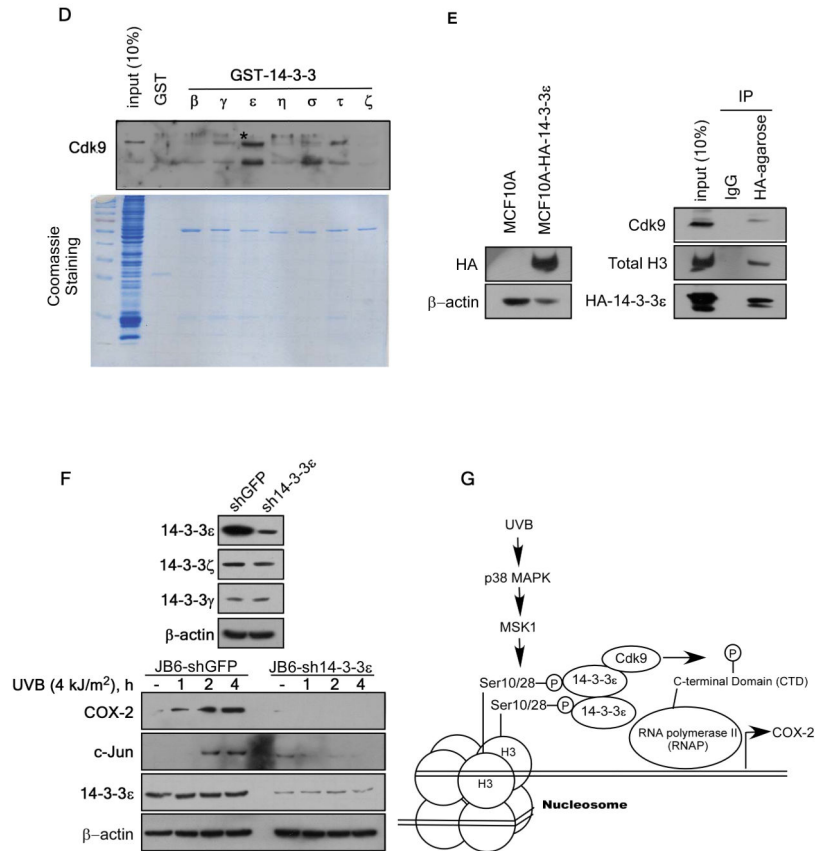


Figure 5.

The 14-3-3 protein isoforms might selectively recognize UVB-induced phosphorylated histone H3 and, particularly, 14-3-3ε plays an important role in UVB-induced COX-2 expression. (A) JB6 cells were either unexposed or exposed to UVB (4 kJ/m²) and harvested after 1 h and total histones were prepared by acid-extraction, followed by TCA precipitation. Purified histones from JB6 cells were mixed overnight with recombinant GST-14-3-3 and immunoprecipitated, using GSH-agarose beads. After washing the beads 3 times, Western blot analysis was conducted to detect total GST and histone H3 proteins. (B) JB6 cells were exposed to UVB (4 kJ/m²) and harvested after 1 h and histone proteins were acid-extracted, followed by TCA precipitation. Total histone proteins extracted from JB6 cells were mixed with recombinant GST-14-3-3 proteins and immunoprecipitated overnight, using GSH-agarose beads. After washing the beads 3 times, Western blotting was conducted to visualize the interaction between the various 14-3-3 isoforms and p-c-Jun, p-p65, p-H3S10, p-H3S28, and total histone H3 (B) or Cdk9 (D). (C) JB6 cell lysates were used to examine the expression changes of the various 14-3-3 isoforms after UVB irradiation. (E) Constitutive expression of retrovirally infected HA-14-3-3ε in MCF10A cells (MCF10A-HA-14-3-3ε) was confirmed by Western blot analysis (left panel). MCF10A-HA-14-3-3ε cells were irradiated with UVB (4 kJ/m²) for 1 h and disrupted with RIPA buffer, containing micrococcal nuclease. The lysates were then immunoprecipitated by HA-resin and washed with RIPA buffer three times. The interaction of HA-14-3-3ε proteins with total H3 or Cdk9 proteins was examined by Western blot (right panel). (F) After establishing JB6 cells, in

which 14-3-3 ϵ was selectively suppressed (left panel), cells were exposed to UVB (4 kJ/m²) and harvested at different times (0, 1, 2, 4 h) and the abundance of COX-2 and c-Jun proteins was assessed by Western blot. (G) A schematic diagram that explains how UVB irradiation induces p38 MAPK/MSK cascade activation, leading to phosphorylation of histone H3 at Ser10 and Ser28 and subsequent recruitment of Cdk9 and RNA polymerase II phosphorylation.

Author Manuscript

Author Manuscript

Author Manuscript

Author Manuscript